


SCIENTIFIC REPORTS



OPEN

Early Detection of Apathetic Phenotypes in Huntington's Disease Knock-in Mice Using Open Source Tools

Shawn Minnig, Robert M. Bragg, Hardeep S. Tiwana, Wes T. Solem, William S. Hovander, Eva-Mari S. Vik, Madeline Hamilton, Samuel R. W. Legg, Dominic D. Shuttleworth, Sydney R. Coffey, Jeffrey P. Cantle & Jeffrey B. Carroll 

Apathy is one of the most prevalent and progressive psychiatric symptoms in Huntington's disease (HD) patients. However, preclinical work in HD mouse models tends to focus on molecular and motor, rather than affective, phenotypes. Measuring behavior in mice often produces noisy data and requires large cohorts to detect phenotypic rescue with appropriate power. The operant equipment necessary for measuring affective phenotypes is typically expensive, proprietary to commercial entities, and bulky which can render adequately sized mouse cohorts as cost-prohibitive. Thus, we describe here a home-built, open-source alternative to commercial hardware that is reliable, scalable, and reproducible. Using off-the-shelf hardware, we adapted and built several of the rodent operant buckets (ROBucket) to test *Htt^{Q111/+}* mice for attention deficits in fixed ratio (FR) and progressive ratio (PR) tasks. We find that, despite normal performance in reward attainment in the FR task, *Htt^{Q111/+}* mice exhibit reduced PR performance at 9–11 months of age, suggesting motivational deficits. We replicated this in two independent cohorts, demonstrating the reliability and utility of both the apathetic phenotype, and these ROBuckets, for preclinical HD studies.

Huntington's disease (HD) is a fatal, progressive neurological disorder caused by a coding cytosine-adenine-guanine (CAG) expansion in the huntingtin (*HTT*) gene, where repeat lengths above 40 result in full penetrance of the disease¹. Patients with HD display a clinical triad of cognitive, psychiatric, and motor symptoms². Although chorea is a prerequisite for formal clinical diagnosis^{3,4} and the most recognized HD related deficit⁵, cognitive and psychiatric symptoms often appear during the prodromal phase of the disease, as many as 10 years prior to the onset of motor dysfunction^{6,7}. Cognitive symptoms in HD include various impairments in learning and memory, deficits in executive function⁸, and difficulty recognizing emotional states^{9,10}, while the most commonly identified psychiatric manifestations include apathy, anxiety, depression, irritability, perseveration, and obsessive behaviors^{6,7,11}.

The cognitive and behavioral aspects of HD contribute to significant declines in functional capacity¹² and are often described as being the most burdensome symptoms to both HD patients and their families¹³. In the absence of effective disease modifying treatments, current therapeutic options for HD are focused on managing these symptoms¹⁴. As such, a great need exists to further study the cognitive and psychiatric components of HD, not only because of the great distress they cause to HD families, but also because understanding the progression of these symptoms will provide researchers with the opportunity to assess the efficacy of potential disease modifying therapies at the earliest time point possible. Unfortunately, given the importance of these phenotypes in HD patients' quality of life, HD preclinical mouse studies do not typically include analysis of impaired cognition and altered affect¹⁵. One potential reason for this is the expense and complexity of the equipment required for traditional cognitive and affective assays, which limits the feasible number of animals in preclinical HD studies. This practical limitation of study size limits the power of HD preclinical studies which, as is common in neuroscience research¹⁶, is generally poor.

Behavioral Neuroscience Program, Department of Psychology, Western Washington University, Bellingham, WA, 98225, United States. Shawn Minnig and Robert M. Bragg contributed equally to this work. Correspondence and requests for materials should be addressed to J.B.C. (email: jeff.carroll@wwu.edu)

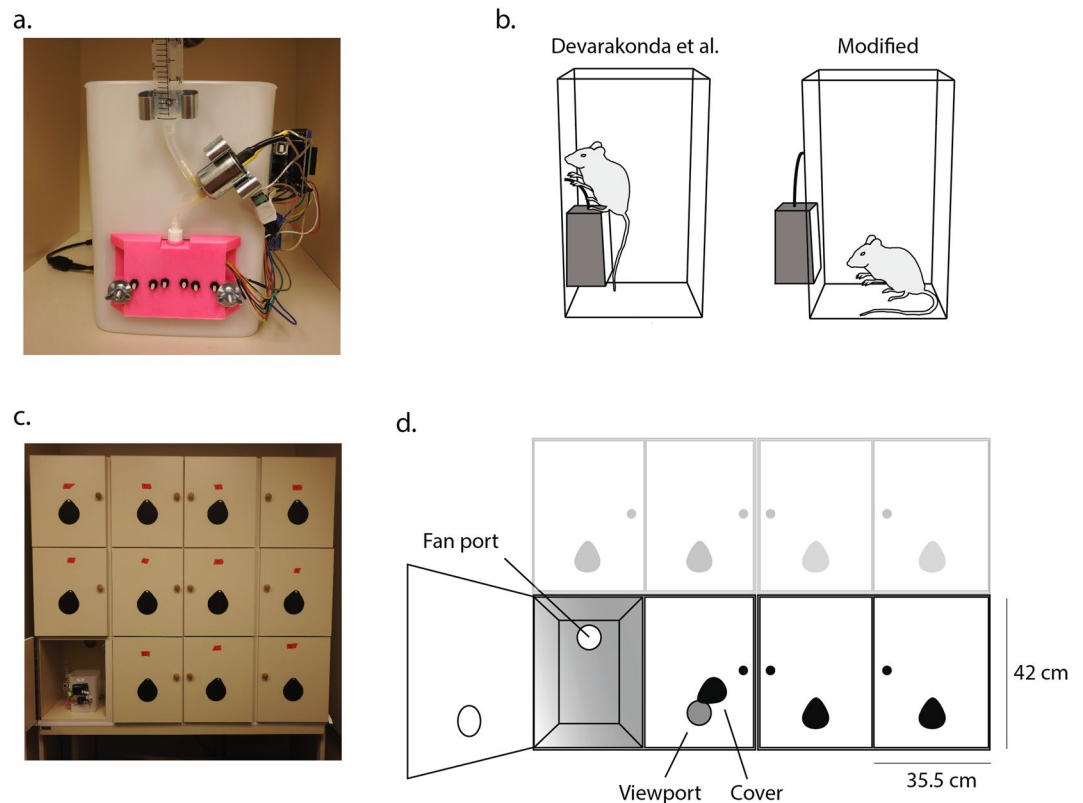


Figure 1. Modified ROBucket design and housing. (a,b) mROBucket with nose-poke housing mounted on the exterior of the bucket reduced time spent exploring the housing and sucrose tubing. (c,d) Construction of a 4 × 3 grid of isolation housing was used to keep each mROBucket independent and facilitate concurrent testing of adequately sized cohorts. Each housing chamber included a small fan for white noise and a viewport to monitor the mROBucket display throughout the experiment.

Amongst HD's psychiatric manifestations, apathy has an extremely high point prevalence, coupled with a uniquely consistent relationship between severity and HD progression^{7,17}. A recent clinical evaluation study of presymptomatic HD mutation carriers found striking increases in the incidence of apathy, even in subjects predicted to be more than 10 years from clinical onset¹⁸. Apathy, as a psychiatric symptom distinct from depression, has been operationalized to contain aspects of diminished motivation, reduced goal-directed behavior, lack of interest in new experiences, and diminished emotional responsivity¹⁹. In HD patients, apathy is correlated with functional capacity and cognition, but not depression, suggesting apathy is a distinctive component of the affective landscape of HD²⁰.

Motivated by the importance of apathy to the lived experience of HD mutation carriers, we are interested in bringing analysis of apathy into HD preclinical studies. Traditional rodent experiments to test motivated behavior include the progressive-ratio (PR) operant task²¹, in which subjects are required to perform increasingly large numbers of nose-pokes or lever-presses to receive a reward. Commercial operant chambers used to assay PR responses in rodents can cost thousands of dollars each, limiting the number of animals (and thereby statistical power) of preclinical studies of apathy. To address this problem, we have modified a recently described open-source operant chamber - the "ROBucket"²² - based on the Arduino computing platform, with a total built cost of approximately \$150/chamber. To validate the modified apparatus, we studied motivation in 9–11 month old B6.*Htt*^{Q111/+} mice, a knock-in mouse model of the HD mutation²³. Using commercially available tools we, and others, have previously observed motivational phenotypes in this model that precede motor or cognitive changes^{24–27}. Using the open-source ROBucket, we confirm specific deficits in progressive, but not fixed, ratio tasks in B6.*Htt*^{Q111/+} mice at this time point, consistent with relatively intact learning but impaired motivation.

Results

Modification of existing operant chamber design. We first precisely recreated a recently reported open source operant chamber ("ROBucket")²². On conducting pilot experiments, we found mice tended to interact with the housing and reward tubing fed through the bucket in the original design. To overcome this distraction, we redesigned the 3D-housing apparatus to be outside the mouse chamber (Fig. 1) - updated plans are available online at <https://zenodo.org/record/101136028>. Studies performed with these modifications revealed that mice quickly learned to interact with the active well to receive 10 μ l of 20% sucrose, and that the modified ROBuckets (mROBucket) accurately counted nose pokes, compared to direct observations.

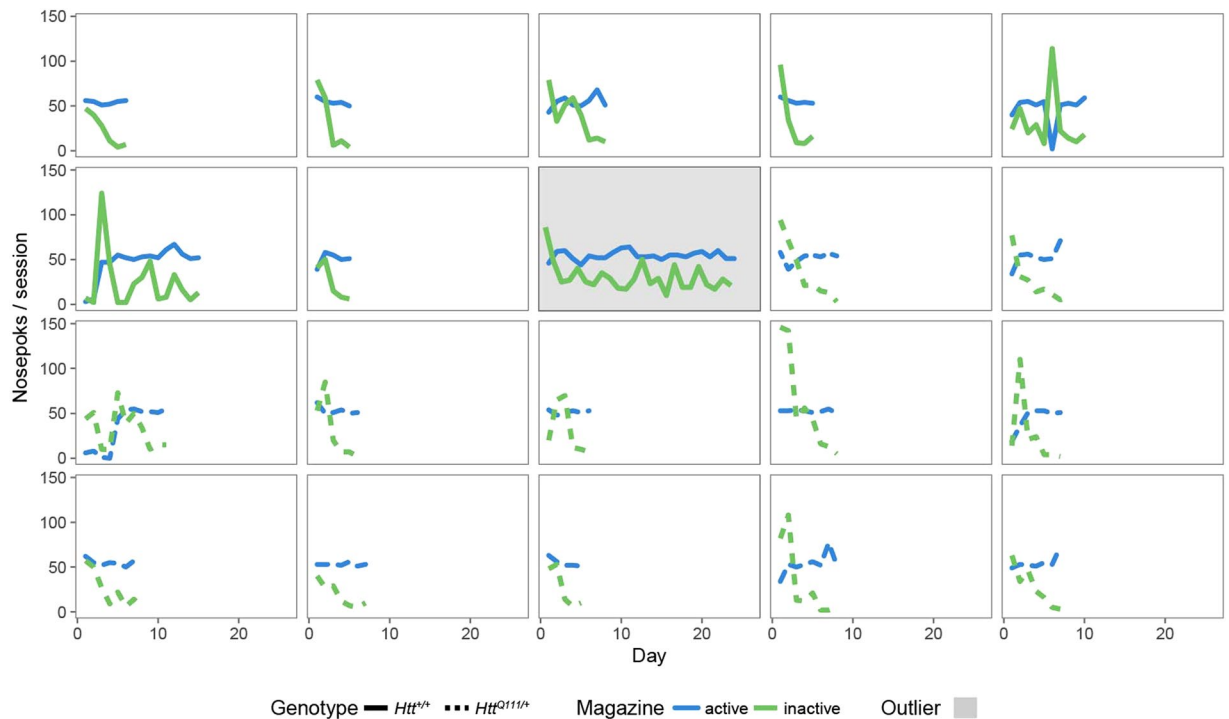


Figure 2. Normal per-mouse acquisition of FR1 task in 10-month-old *Htt^{Q111/+}* mice. Shown for each mouse is the number of nose pokes per 1 hour session in the active (blue) and inactive (green) wells. *Htt^{+/+}* mice ($n = 8$) are graphed with solid lines, *Htt^{Q111/+}* with dashed lines ($n = 12$). One mouse (grey highlight) was excluded for failing to pass the pre-defined FR1 acquisition criteria.

Normal fixed ratio performance in *Htt^{Q111/+}* mice. 9-month-old male B6.*Htt^{+/+}* ($n = 8$) and B6.*Htt^{Q111/+}* ($n = 12$) mice (hereafter *Htt^{+/+}* and *Htt^{Q111/+}*) were single-housed and food restricted over 2 weeks (target weight loss of 2%/day, final body weight ~85% free-feeding weight) before operant testing. We observed no impact of genotype on baseline body weight or the rate at which *Htt^{+/+}* and *Htt^{Q111/+}* mice lost weight during food restriction (Supplemental Fig. 1). After body weight stabilized, mice were placed into mROBucket chambers for 1 hour sessions each day on a fixed ratio 1 (FR1) reinforcement schedule - i.e. one nose poke in the active well resulted in sucrose delivery in the reward well. There was a 1 second timeout after each active well response. Two criteria were required for progression to the next phase: a 3:1 preference for the active well versus the inactive well and 20 or more reinforcements for 3 consecutive days. All mice, with the exception of a single *Htt^{+/+}* mouse (Fig. 2, grey panel), quickly learned the task (Fig. 3, average time to FR1 criteria 7.5 ± 2.4 days).

We observed no effect of genotype on days to meet criteria, the active/inactive nose poke ratio, or total nose pokes per session on the FR1 task (Fig. 3). This suggests 9-month-old male *Htt^{Q111/+}* mice are able to normally acquire this simple discrimination task.

After meeting both criteria for FR1, we next trained the mice on a fixed ratio 5 (FR5) task for 3 days to familiarize them with tasks requiring multiple nose pokes to achieve reward. There was a 1 second timeout after each active well response. Consistent with the FR1 task, 9-month-old male *Htt^{Q111/+}* mice are able to normally acquire this simple discrimination task, with no differences observed between the ratio of active/inactive well responses or the total number of nose pokes per session (Fig. 4). This suggests fatigue and motor dysfunction do not prevent *Htt^{Q111/+}* mice from making large numbers of accurate nose pokes in an hour-long session (average of 273.1 ± 11.7 nose pokes/session).

Reduced progressive ratio performance in *Htt^{Q111/+}* mice. Regardless of performance, mice were advanced to a progressive ratio (PR) task after 3 days of FR5 training. The PR task requires the animals to respond with an exponentially increasing number of sequential nose pokes in the active well to receive the reward (1, 2, 4, 6, 9, 12, etc., according to the formula $R = \lfloor 5e^{(N^{0.2})} \rfloor - 5$)²⁹. The final number of reinforcements achieved is referred to as the “breakpoint”²¹. We established the criterion for the PR task based on breakpoint stabilization, or less than 10% variation in the breakpoint in trials over 3 consecutive days. Both *Htt^{+/+}* and *Htt^{Q111/+}* mice learned the PR task, with breakpoints stabilizing between 4–17 days.

We observed no genotype effect on the days to criterion (Fig. 5a) or average active/inactive ratio (Fig. 5b) during the PR task, however *Htt^{Q111/+}* mice perform significantly fewer total nose pokes per session (44% reduction, Fig. 5c) and consequently receive fewer rewards per session (17% reduction). This results in a 37% reduction in the final stabilized breakpoint of *Htt^{Q111/+}* mice compared to *Htt^{+/+}* mice (Fig. 5d). Post-hoc analysis suggests our experiment had 94.6% power to detect a breakpoint difference between genotypes ($n = 7$ *Htt^{+/+}* and 12 *Htt^{Q111/+}*; effect size, $d = 1.8$, type 1 error probability = 0.05).

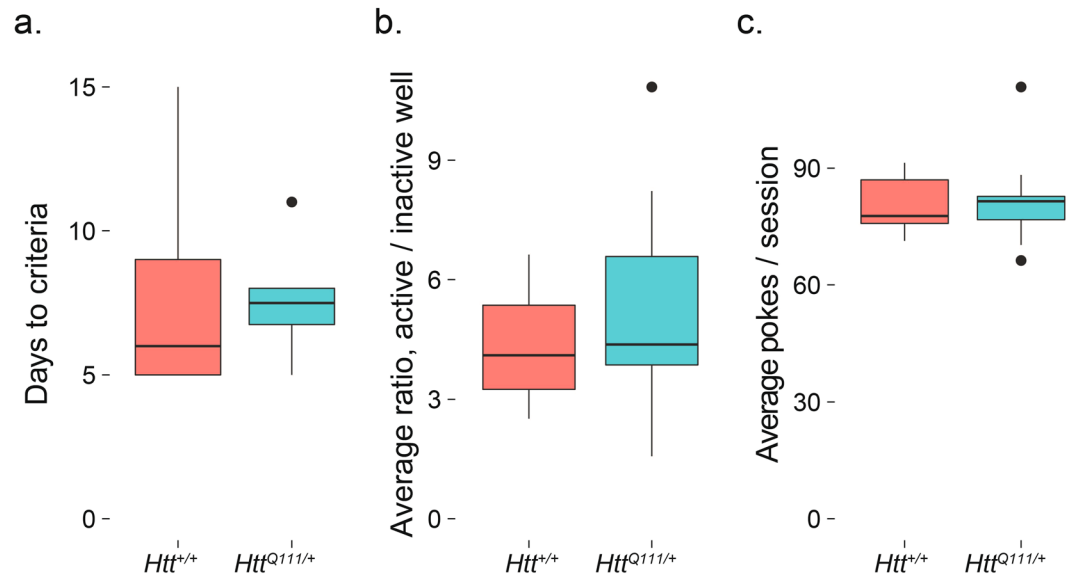


Figure 3. Normal performance of FR1 task in 10-month-old male *Htt*^{Q111/+} mice. No genotype effect is observed in the days to criteria (a). $t_{(7,1)} = 0.2, p = 0.8$, active/inactive well ratio (b). $t_{(16,9)} = -0.9, p = 0.4$ or average total nose pokes per session (c). $t_{(16,5)} = -0.1, p = 0.9$. Horizontal lines in the boxes indicate 25th, 50th and 75th percentiles, while vertical lines indicate 1.5 times the interquartile range; outliers beyond these values are graphed as points.

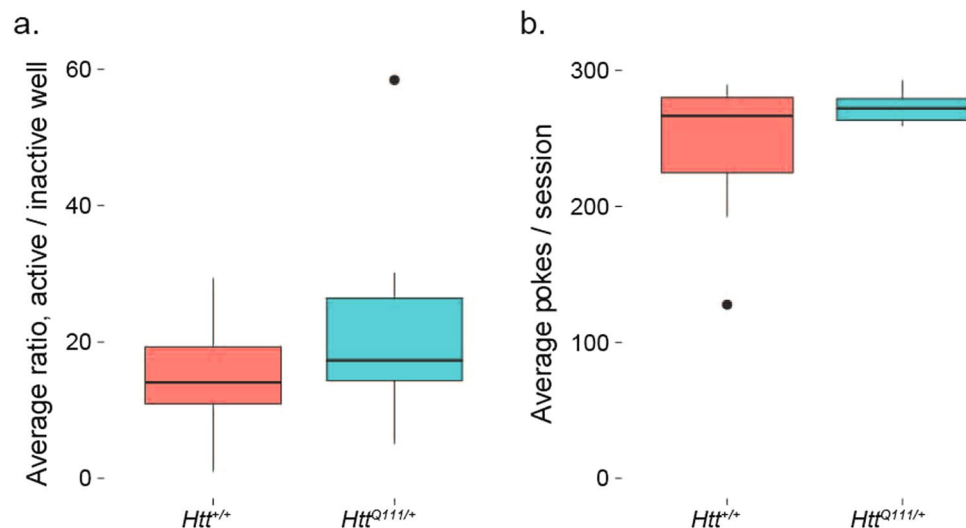


Figure 4. Normal performance of FR5 task in 10-month-old *Htt*^{Q111/+} mice. No genotype effect is observed in the active/inactive well ratio (a). $t_{(16,6)} = -1.3, p = 0.2$ or average total nose pokes per session (b). $t_{(6,3)} = -1.4, p = 0.2$; $n = 7$ *Htt*^{+/+}, 12 *Htt*^{Q111/+}. Horizontal lines in the boxes indicate 25th, 50th and 75th percentiles, while vertical lines indicate 1.5 times the interquartile range; outliers beyond these values are graphed as points.

Replication in an independent cohort. We are interested in the improvement of preclinical trials in HD, particularly their reproducibility^{27,30–32}. To determine whether the mROBucket apparatus and progressive ratio task are reproducible assays of motivated behavior, we repeated the experiment in a new cohort of similarly aged (10–11 months) male *Htt*^{+/+} ($n = 12$) and *Htt*^{Q111/+} mice ($n = 12$). Consistent with the findings of our first cohort, we observe no effect of genotype on the total number of nose pokes in the FR1 task (Fig. 6a). Similarly, in the FR5 task, *Htt*^{Q111/+} mice perform equivalently to *Htt*^{+/+} mice for total nose pokes (Fig. 6b). In the PR task, *Htt*^{Q111/+} displayed reduced total pokes ($t_{(17,1)} = 3.9, p < 0.001$), earned fewer rewards ($t_{(21,5)} = 3.9, p < 0.001$) and displayed a 46% reduction in final breakpoint (Fig. 6c). Post-hoc analysis of the replication cohort ($n = 12$ *Htt*^{+/+} and 12 *Htt*^{Q111/+}, effect size, $d = 1.6$, type 1 error probability = 0.05) indicates we achieved 96.3% power.

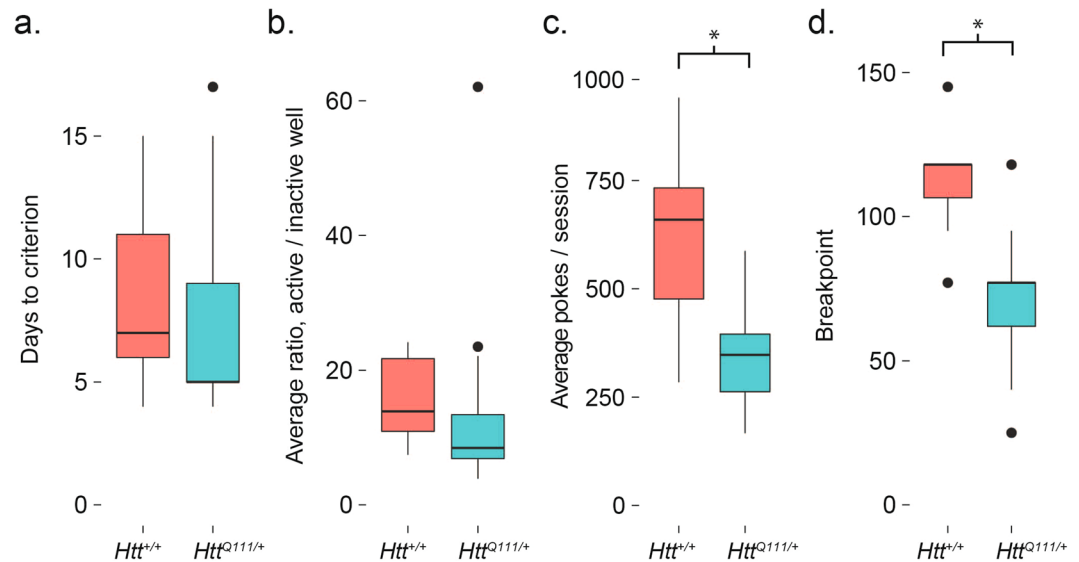


Figure 5. Progressive ratio deficits in 10-month-old *Htt*^{+/+} and *Htt*^{Q111/+} mice. No genotype effect is observed in (a) the final days to criterion ($t_{(14,3)} = 0.5$, $p = 0.6$), or (b) active/inactive well ratio ($t_{(15,8)} = 0.3$, $p = 0.8$) during the PR task. However, *Htt*^{Q111/+} mice do have (c) reduced total nose pokes ($t_{(7,8)} = 3.0$, $p = 0.02$), reduced rewards/session ($t_{(12,1)} = 3.0$, $p = 0.01$) and a consequently (d) reduced final breakpoint ($t_{(13,9)} = 4.0$, $p = 0.002$) during the PR task. *Indicates $p < 0.05$. Horizontal lines in the boxes indicate 25th, 50th and 75th percentiles, while vertical lines indicate 1.5 times the interquartile range; outliers beyond these values are graphed as points.

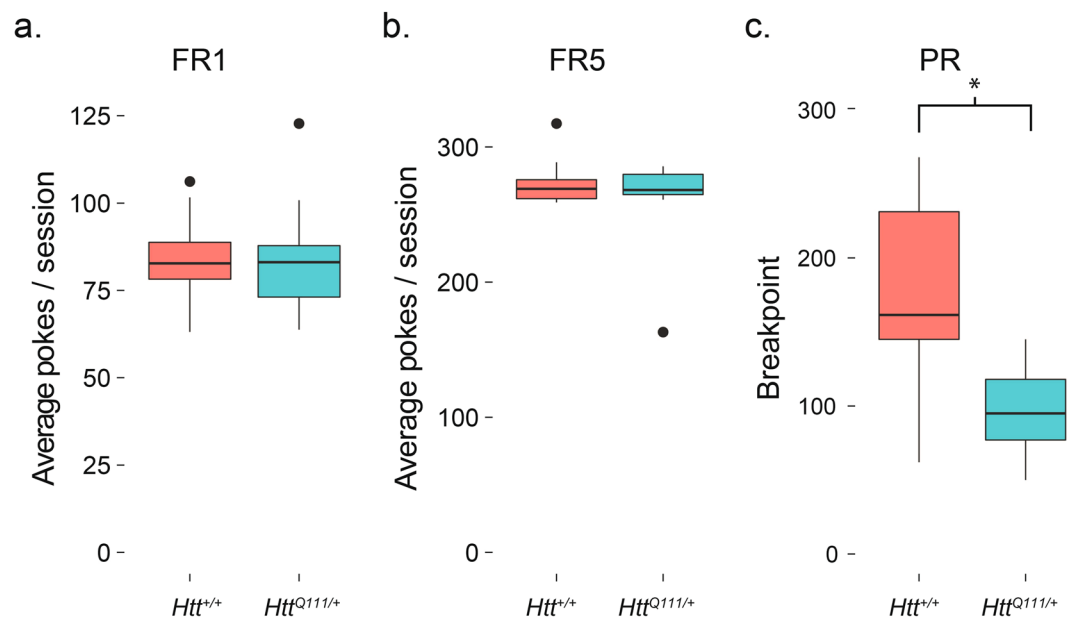


Figure 6. Independent replication of progressive ratio deficits in 10-month-old *Htt*^{+/+} and *Htt*^{Q111/+} mice. (a) We observed no difference in the total nose pokes during the FR1 task ($t_{(19,8)} = 0.12$, $p = 0.9$). (b) Similarly, in the FR5 task, *Htt*^{Q111/+} mice perform equivalently to *Htt*^{+/+} mice ($t_{(16,3)} = 0.9$, $p = 0.4$). (c) The replication cohort had a significantly reduced final breakpoint ($t_{(16,2)} = 3.9$, $p = 0.001$) in the PR task. *Indicates $p < 0.05$. Horizontal lines in the boxes indicate 25th, 50th and 75th percentiles, while vertical lines indicate 1.5 times the interquartile range; outliers beyond these values are graphed as points.

Discussion

Apathy is a core feature of affective dysfunction in HD¹⁷, but analysis of apathy and other affective disturbances is rarely included in preclinical studies of HD³³. Here, we demonstrate that an inexpensive open source apparatus can robustly and reproducibly detect motivational deficits in 9–11 month old *Htt*^{Q111/+} mice. These motivational deficits precede overt motor, cognitive, or neurodegenerative changes in this model²⁷, suggesting they may occur amongst the earliest changes associated with mutant huntingtin expression *in vivo*. A recent study from

the Yhnell *et al.* tested *Htt*^{Q111/+} mice in commercial operant boxes at 6-, 12-, and 18-months of age²⁴, finding that *Htt*^{Q111/+} mice showed no deficits in fixed ratio testing at 6- or 12-months, but had reduced breakpoint in progressive ratio at 12 months when delivering similar volumes of liquid reward to those used in our study (7.5 μ L vs. 10 μ L used in our study). While differences in the methodology for the training, progressive ratio task, and breakpoint determination between our study and the Yhnell *et al.* study limit direct comparison, our results confirm those found in the commercial apparatus: that there are no deficits in fixed ratio testing at a time point between the 6- and 12-month timepoints (9- and 10-mo for our independent cohorts, respectively), while we also confirm the significant progressive ratio deficits found in the commercial apparatus at 12-months in our slightly younger cohorts tested using open-source equipment.

The basal ganglia, and particularly the striatum, are the most strikingly impacted brain regions in Huntington's disease, showing robust volume declines many years before clinical disease onset^{7,34}. While no full-length HD mouse models experience similar pronounced neurodegeneration, a number of imaging^{30,35,36} and molecular analyses³⁷ confirm that the caudoputamen is the most strikingly impacted brain region in mice expressing mutant *Htt*. In humans, focal ischemic basal ganglia damage is associated with a range of motivational deficits³⁸, including notable deficits in incentive motivation - the process of activating specific behavioral responses based on predicted reward³⁹. In stroke patients with basal ganglia lesions, deficits in incentive motivation occur in the absence of deficits in hedonic responses, consistent with reduced progressive ratio performance in *Htt*^{Q111/+} mice (here, and^{24,27}) at a time when sucrose preference tasks suggest no alterations in hedonic drive in these mice²⁷. Changes in instrumental motivation may therefore serve as a translatable readout of basal ganglia dysfunction in mice. The deficits in instrumental motivation seen here may provide a behavioral tool for quantifying this dysfunction, however we caution that mouse behavioral phenotypes likely map imperfectly onto complex symptoms - such as apathy - in human HD patients.

Statistical power in neuroscience studies, and especially behavioral studies, is generally low¹⁶, leading to widespread calls for improvements in conducting and reporting of preclinical work⁴⁰. While the use of operant chambers can improve preclinical studies by automating data collection of complex behavioral tasks, these benefits can be negated by the cost of the apparatus. Traditional operant chambers from commercial suppliers cost thousands of dollars, placing a practical limit on the number of mice that can be screened in parallel in a single lab and thereby limiting the power of these studies. Recent technological developments - including the rapid development of inexpensive additive manufacturing (i.e. "3D printing") and low-cost open source computing platforms (e.g. Raspberry Pi and Arduino) - enable open source alternatives to commercial products. Further, they allow for rapid design and software modifications to assay behavior through multiple paradigms. These tools have been applied to video tracking of behavior⁴¹, integrated microscopy, temperature control, and optogenetics in small animal experiments⁴², as well as the rodent operant chambers used here²². These technologies render practical the fabrication of a large number of chambers (12 were used in the current study), so dozens of mice can be tested in parallel in a single lab, with a limited number of handlers.

These experiments confirm previous findings that motivational deficits occur before pronounced neurodegeneration in the *Htt*^{Q111/+} model of HD. They also show that these deficits are assayable using inexpensive hardware and open source software tools, which should enable their more widespread utilization in preclinical studies in HD.

Methods

Mouse. B6.*Htt*^{Q111} mice, which have been previously described⁴³, were originally obtained from JAX (Research Resource Identifier: IMSR_JAX:003456) and bred and maintained at the Western Washington University vivarium. Mice were group housed until 9–10 months of age and given access to food and water *ad libitum*, until two weeks before testing was to begin. For genotyping, presence or absence of the mutant allele was determined by polymerase chain reaction of DNA using the primers CAG1 (5'-ATGAAGGCCTTCGAGTCCCTCAAGTCCTTC-3')⁴⁴ and HU3 (5'-GGCGGCTGAGGAAGCTGAGGA-3')⁴⁵. All experiments were conducted in accordance to the NIH Guide for the Care and Use of Laboratory Animals and approved by the Western Washington University animal care and use committee (protocol 16-007).

Apparatus. 2-choice operant chambers were constructed according to the design from Devarakonda²² with modifications. Briefly, Arduino-controlled operant boxes deliver a liquid sucrose reward in response to nose-pokes with various reinforcement schedules. The apparatus here was modified to place the nose-poke photo-beam housing on the outer, rather than inner, wall of the operant chamber (see Fig. 1b). This eliminated time spent exploring the nose-poke housing and associated tubing, and resulted in cleaner acquisition of the FR/PR tasks. Isolation housing was designed and constructed as a grid of 3 \times 4 chambers (35 \times 42 \times 42 cm each) with view ports in the front to visualize the response readings and vent fans in the back to produce white noise (Fig. 1d).

Behavioral Testing. Mice were single-housed and fasted over two weeks to reduce body weight to 85% of free feeding weight prior to testing and maintained at this weight for the duration of testing. For FR1 testing, mice learned to nose-poke on a fixed-ratio reinforcement schedule where a single nose-poke in the active well elicits delivery of a sucrose reward (10 μ L, 20% sucrose), with a 1-second timeout after each active well press. Trial duration was 60 minutes or until the subject received 50 reinforcements, at which point mice were promptly removed. Acquisition criteria for the FR1 schedule were met when mice exhibited discrimination criteria of $\geq 3:1$ for the active:inactive well and received ≥ 20 reinforcements for 3 consecutive days. Mice not meeting the FR1 acquisition criteria by 17 days were excluded from further testing (this occurred in 1 mouse from each cohort, or approximately 5% of mice). After meeting FR1 criteria, mice were moved to FR5 testing, where the reinforcement schedule requires five pokes to earn 1 reward, for three consecutive days.

For PR testing, mice were tested on a progressive ratio schedule of reinforcement where the number of nose pokes required to elicit reinforcement is calculated using the equation $\text{Reinforcements} = \lfloor 5e^{(N \times 0.2)} \rfloor - 5$, where N is equal to the number of sucrose solution reinforcements already earned plus 1. When mice earned the same number of rewards ($\pm 10\%$, or within 1 if less than 10 rewards are earned) for 3 consecutive days, they were considered stabilized at their “breakpoint.” For full methods and instructions, see published online methods at <https://zenodo.org/record/101136028>.

Statistical analysis. All data were processed using R statistical software⁴⁶. Welch’s t -tests were used to correct for unequal variances, linear mixed effects ANOVAs were run using the ‘nlme’ package⁴⁷, effect size was calculated with the ‘compute.es’ package⁴⁸, and power was calculated using the ‘pwr’ package⁴⁹. Graphics were produced using ‘ggplot2’⁵⁰ and Illustrator (Adobe).

References

- MacDonald, M. E. *et al.* A novel gene containing a trinucleotide repeat that is expanded and unstable on Huntington’s disease chromosomes. *Cell* **72**, 971–983 (1993).
- Walker, F. O. *Huntington’s disease*. **369**, 218228 (2007).
- Loy, C. T. & McCusker, E. A. Is a motor criterion essential for the diagnosis of clinical huntington disease? *PLoS Curr.* **5** (2013).
- Reilmann, R., Leavitt, B. R. & Ross, C. A. Huntington’s disease: A field on the move. *Mov. Disord.* **29**, 1333–1334 (2014).
- Papoutsi, M., Labuschagne, I., Tabrizi, S. J. & Stout, J. C. The cognitive burden in Huntington’s disease: pathology, phenotype, and mechanisms of compensation. *Mov. Disord.* **29**, 673–683 (2014).
- Epping, E. A. *et al.* Longitudinal Psychiatric Symptoms in Prodromal Huntington’s Disease: A Decade of Data **173**, 184–192 (2016).
- Tabrizi, S. J. *et al.* Predictors of phenotypic progression and disease onset in premanifest and early-stage Huntington’s disease in the TRACK-HD study: analysis of 36-month observational data. *Lancet Neurol.* **12**, 637–649 (2013).
- Giralt, A., Saavedra, A., Alberch, J. & Pérez-Navarro, E. Cognitive Dysfunction in Huntington’s Disease: Humans, Mouse Models and Molecular Mechanisms. *J. Huntingtons Dis.* **1**, 155–173 (2012).
- Labuschagne, I. *et al.* Emotional face recognition deficits and medication effects in pre-manifest through stage-II Huntington’s disease. **207**, 118–126 (2013).
- Novak, M. J. U. *et al.* Altered brain mechanisms of emotion processing in pre-manifest Huntington’s disease. *Brain* **135**, 1165–1179 (2012).
- Craufurd, D., Thompson, J. C. & Snowden, J. S. *Behavioral changes in Huntington Disease* **14**, 219–226 (2001).
- Nehl, C. & Paulsen, J. S. & Huntington Study Group. Cognitive and psychiatric aspects of Huntington disease contribute to functional capacity. *J. Nerv. Ment. Dis.* **192**, 72–74 (2004).
- Paulsen, J. S. Cognitive impairment in Huntington disease: diagnosis and treatment. *Curr. Neurol. Neurosci. Rep.* **11**, 474–483 (2011).
- Frank, S. Treatment of Huntington’s disease. *Neurotherapeutics* **11**, 153–160 (2014).
- Menalled, L. *et al.* Systematic behavioral evaluation of Huntington’s disease transgenic and knock-in mouse models. **35**, 319–336 (2009).
- Button, K. S. *et al.* Power failure: why small sample size undermines the reliability of neuroscience. *Nat. Rev. Neurosci.* **14**, 365–376 (2013).
- Eddy, C. M., Parkinson, E. G. & Rickards, H. E. Changes in mental state and behaviour in Huntington’s disease. *Lancet Psychiatry* **3**, 1079–1086 (2016).
- Martinez-Horta, S. *et al.* Neuropsychiatric symptoms are very common in premanifest and early stage Huntington’s Disease. *Parkinsonism Relat. Disord.* **25**, 58–64 (2016).
- Starkstein, S. E. & Leentjens, A. F. G. The nosological position of apathy in clinical practice. *J. Neurol. Neurosurg. Psychiatry* **79**, 1088–1092 (2008).
- Naarding, P., Janzing, J. G. E., Eling, P., van der Werf, S. & Kremer, B. Apathy is not depression in Huntington’s disease. *J. Neuropsychiatry Clin. Neurosci.* **21**, 266–270 (2009).
- Hodos, W. Progressive ratio as a measure of reward strength. <https://doi.org/10.1126/science.134.3483.943> (1961).
- Devarakonda, K., Nguyen, K. P. & Kravitz, A. V. ROBucket: A low cost operant chamber based on the Arduino microcontroller. 1–7 (2015).
- Wheeler, V. C. *et al.* Long glutamine tracts cause nuclear localization of a novel form of huntingtin in medium spiny striatal neurons in HdhQ92 and HdhQ111 knock-in mice. *Hum. Mol. Genet.* **9**, 503–513 (2000).
- Yhnell, E., Dunnett, S. B. & Brooks, S. P. A Longitudinal Operant Assessment of Cognitive and Behavioural Changes in the HdhQ111 Mouse Model of Huntington’s Disease. *PLoS One* **11**, e0164072 (2016).
- Oakeshott, S. *et al.* A mixed fixed ratio/progressive ratio procedure reveals an apathy phenotype in the BAC HD and the z_Q175 KI mouse models of Huntington’s disease. <https://doi.org/10.1371/4f972cffe82c0> (2012).
- Covey, D. P., Dantrassy, H. M., Zlebnik, N. E., Gildish, I. & Cheer, J. F. Compromised Dopaminergic Encoding of Reward Accompanying Suppressed Willingness to Overcome High Effort Costs Is a Prominent Prodromal Characteristic of the Q175 Mouse Model of Huntington’s Disease. **36**, 4993–5002 (2016).
- Bragg, R. M. *et al.* Motivational, proteostatic and transcriptional deficits precede synapse loss, gliosis and neurodegeneration in the B6.Htt^{+/+}Q111^{+/+} model of Huntington’s disease. *Sci. Rep.* **7**, 41570 (2017).
- Bragg, R. & Minnig, S. *Carroll. Modified ROBucket design.* <https://doi.org/10.5281/zenodo.1011360> (2017).
- Richardson, N. R. & Roberts, D. C. Progressive ratio schedules in drug self-administration studies in rats: a method to evaluate reinforcing efficacy. *J. Neurosci. Methods* **66**, 1–11 (1996).
- Carroll, J. B. *et al.* Natural history of disease in the YAC128 mouse reveals a discrete signature of pathology in Huntington disease. **43**, 257–265 (2011).
- Lerch, J. P. *et al.* Automated deformation analysis in the YAC128 Huntington disease mouse model. **39**, 3239 (2008).
- Coffey, S. R. *et al.* Peripheral huntingtin silencing does not ameliorate central signs of disease in the B6.HttQ111^{+/+} mouse model of Huntington’s disease. *PLoS One* **12**, e0175968 (2017).
- Menalled, L. & Brunner, D. Animal models of Huntington’s disease for translation to the clinic: Best practices. *Mov. Disord.* **29**, 1375–1390 (2014).
- Paulsen, J. S. *et al.* Detection of Huntington’s disease decades before diagnosis: the Predict-HD study. *J. Neurol. Neurosurg. Psychiatry* **79**, 874–880 (2008).
- Sawiak, S. J., Wood, N. I., Williams, G. B., Morton, A. J. & Carpenter, T. A. Voxel-based morphometry with templates and validation in a mouse model of Huntington’s disease. *Magn. Reson. Imaging* **31**, 1522–1531 (2013).
- Heikkinen, T. *et al.* Characterization of Neurophysiological and Behavioral Changes, MRI Brain Volumetry and 1H MRS in zQ175 Knock-In Mouse Model of Huntington’s Disease. **7** (2012).
- Langfelder, P. *et al.* Integrated genomics and proteomics define huntingtin CAG length-dependent networks in mice. <https://doi.org/10.1038/nn.4256> (2016).
- Levy, R. & Czernacki, V. Apathy and the basal ganglia. *J. Neurol* **253**(Suppl 7), VII54–61 (2006).

39. Schmidt, L. *et al.* Disconnecting force from money: effects of basal ganglia damage on incentive motivation. *Brain* **131**, 1303–1310 (2008).
40. Landis, S. C. *et al.* A call for transparent reporting to optimize the predictive value of preclinical research. *Nature* **490**, 187–191 (2012).
41. Nashaat, M. A. *et al.* Pixying Behavior: A Versatile Real-Time and Post Hoc Automated Optical Tracking Method for Freely Moving and Head Fixed Animals. *eNeuro* **4** (2017).
42. Maia Chagas, A., Prieto-Godino, L. L., Arrenberg, A. B. & Baden, T. The €100 lab: A 3D-printable open-source platform for fluorescence microscopy, optogenetics, and accurate temperature control during behaviour of zebrafish, *Drosophila*, and *Caenorhabditis elegans*. *PLoS Biol.* **15**, e2002702 (2017).
43. Wheeler, V. C. *et al.* Length-dependent gametic CAG repeat instability in the Huntington's disease knock-in mouse. *Hum. Mol. Genet.* **8**, 115–122 (1999).
44. Mangiarini, L. *et al.* Instability of highly expanded CAG repeats in mice transgenic for the Huntington's disease mutation. *Nat. Genet.* **15**, 197–200 (1997).
45. Riess, O., Noerremoele, A., Soerensen, S. A. & Epplen, J. T. Improved PCR conditions for the stretch of (CAG)_n repeats causing Huntington's disease. *Hum. Mol. Genet.* **2**, 637–637 (1993).
46. R Core Team. R: A language and environment for statistical computing. R Foundation for Statistical Computing. *R-project* Available at: <https://www.R-project.org/>. (Accessed: 2017)
47. Pinheiro J., Bates D., DebRoy S., Sarkar D. & R. Core Team. `nlme: Linear and Nonlinear Mixed Effects Models`. R package version 3.1–131. *R-project* Available at <https://CRAN.R-project.org/package=nlme> (2017).
48. Del Re, A. C. `compute.es: Compute Effect Sizes`. R package version 0.2-2. *R-project* Available at: <http://cran.r-project.org/web/packages/compute.es> (2013).
49. Champely, S. `pwr: Basic Functions for PowerAnalysis`. R-project Available at: <https://CRAN.R-project.org/package=pwr> (2017).
50. Wickham, H. *ggplot2: Elegant Graphics for Data Analysis*. (Springer, 2016).

Acknowledgements

This work was supported by funding from the Western Washington University Behavioral Neuroscience Program. The authors would like to thank Dr. Janet Finlay for her protocol to reduce mouse body weight for the behavior experiments and Jim Mullen and Jason Bryenton for technical assistance with the design and building of isolation housing.

Author Contributions

S.M. and R.M.B. worked together to devise the experiments, modify the behavioral apparatus, analyze the data, and prepare the manuscript and should be considered co-first authors. S.M., H.S.T., W.T.S., E.M.V., M.H., S.R.W.L., D.D.S., and S.R.C. collected the data for the initial behavior cohort. H.S.T., W.T.S., R.M.B., and S.M. planned and collected the data with W.S.H. for the replication cohort. J.P.C. and J.B.C. planned and supervised the experiments.

Additional Information

Supplementary information accompanies this paper at <https://doi.org/10.1038/s41598-018-20607-7>.

Competing Interests: The authors declare that they have no competing interests.

Publisher's note: Springer Nature remains neutral with regard to jurisdictional claims in published maps and institutional affiliations.



Open Access This article is licensed under a Creative Commons Attribution 4.0 International License, which permits use, sharing, adaptation, distribution and reproduction in any medium or format, as long as you give appropriate credit to the original author(s) and the source, provide a link to the Creative Commons license, and indicate if changes were made. The images or other third party material in this article are included in the article's Creative Commons license, unless indicated otherwise in a credit line to the material. If material is not included in the article's Creative Commons license and your intended use is not permitted by statutory regulation or exceeds the permitted use, you will need to obtain permission directly from the copyright holder. To view a copy of this license, visit <http://creativecommons.org/licenses/by/4.0/>.

© The Author(s) 2018